Revised Implementation of the Green-Ampt Infiltration Method in TELEMAC-2D

Leon Frederik De Vos[1], Karl Broich[2], Moritz Wirthensohn[2], Nils Rüther[1]
Frederik.de-vos@tum.de, Munich, Germany
[1]: TUM, Chair of Hydraulic Engineering
[2]: TUM, Chair of Hydrology and River Basin Management

***Abstract* – The Green-Ampt method, widely utilized for rainfall-runoff modeling, describes the infiltration process based on soil parameters and rain event characteristics. This method has been integrated into Telemac-2D since v8p4 using an explicit integral approach. Yet its current implementation has not been thoroughly tested. We compare the current implementation with our revised implementations based on the Serrano and the Sadeghi solutions. The revised implementations calculate the ponding time at each node and timestep, considering a time-variant rain intensity based on the method by Chu. The revised implementations furthermore allow inundated water to infiltrate the soil even after the rain event, enabling the model to drain impounded areas. Consequently, the revised implementations affect not only the infiltration calculation but also impact water depths and simulated hydrographs during flood event modeling on a catchment scale. In this study, we present revised implementations of the Green-Ampt method in Telemac-2D and compare their performances against the current version. We compare two test cases: the validation example "pluie" and a catchment in Germany. Based on the results of this study, we recommend using the explicit solution by Sadeghi.**

Keywords: TELEMAC 2D, Rainfall, Runoff, Green-Ampt, Flood

I. Introduction

With the advancement of computational resources, flood modeling is no longer constrained by the need for external coupling between hydrologic and hydrodynamic models. Modern hydrodynamic models now have the capacity to directly incorporate hydrologic processes as source terms, enabling solving the shallow water equations (SWE) across entire catchments. Ligier [1] was the first to implement a rainfall-runoff model in TELEMAC, establishing the "pluie" validation case. The Soil Conservation Service Curve Number (SCS-CN) method, which was implemented in this context, is widely utilized due to its accessibility and minimal input data requirements [2]. However, the SCS-CN method offers a highly simplified representation of the rainfall-runoff process, particularly as it does not account for soil re-infiltration after a rain event. Consequently, alternative rainfall-runoff models have also been integrated into TELEMAC.

Broich et al. [3] introduced an initial version of the implicit Green-Ampt infiltration model [4], based on the explicit Serrano approximation [5] for constant rainfall. Travert et al. [6] implemented the Horton infiltration model as well as an integral solution of the Green-Ampt infiltration model, with their contributions being released in TELEMAC v8p4. However, their implementation was not tested on a real application and does not support infiltration after the rain event. Both the initial implementation by Broich et al. and the released implementation by Travert et al. allow for a spatially variable hydraulic conductivity, while other soil parameters remain spatially constant.

In this study, we present the following implementations, revisions, and extensions of the Green-Ampt infiltration method:

- An explicit solution of the Green-Ampt method by Sadeghi et al. [7] utilizing the method of Chu [8] for unsteady rainfall.
- An explicit solution of the Green-Ampt method by Serrano, also employing the method of Chu for unsteady rainfall.
- An extension of the implementation of Travert et al., enabling infiltration after the rain event
- An extension of the Green-Ampt method in TELEMAC to allow for multiple spatially variable soil parameters.

We begin by providing a detailed explanation of the Green-Ampt infiltration method, along with its approximations and implementations in TELEMAC. We then present the results of these different implementations using the *"pluie"* validation case. Finally, we apply these implementations to a flood model of an isolated catchment in central Germany. We outline the steps of model generation and compare the performance of the different Green-Ampt infiltration method implementations.

II. Green-Ampt Infiltration Method

The Green-Ampt infiltration method calculates the infiltration rate f [m/s] based on the cumulative infiltrated water F [m] and different soil parameters [4]:

$$f(t) = K_S[1 + \frac{\Psi_f(\theta_s - \theta_i)}{F(t)}] \quad (1)$$

Where K_S [m/s] is the hydraulic conductivity, Ψ_f [m] is the suction head, θ_i [-] is the initial water content and θ_s is the saturated water content.

Mein and Larson [9] divide the infiltration during a rain event into two distinct periods. The first period extends from the start of the rain event until the ponding time, t_P. During this period, all rainfall infiltrates into the soil. After the ponding time, the infiltration rate is calculated using equation (1) and surface runoff begins to form. If the rain intensity (RI [m/s]) is less than the hydraulic conductivity, ponding conditions are not reached. For constant rain intensity, the ponding time can be calculated as follows:

$$t_P = \frac{\frac{\Psi_f(\theta_s-\theta_i)K_S}{RI-K_S}}{RI} \quad (2)$$

For unsteady rain intensity, calculating the ponding time becomes more complex, as it depends on the current rain intensity as well as the cumulative rainfall from previous periods. Chu [8] addresses this by dividing a rain event into intervals of constant intensity, which is a common representation in hyetographs. Equation (2) can thus be extended to account for unsteady rain:

$$t_{PUR} = \frac{\frac{\Psi_f(\theta_s-\theta_i)K_S}{RI-K_S}-P(t_{n-1})}{RI} + t_{n-1} \quad (3)$$

Where t_{n-1} is the initial time of a constant intensity period and P is the cumulative rainfall.

The following sections detail the implementation of the different solutions in TELEMAC. The adapted subroutine is "*runoff_greenampt.f*".

A. Implementation of the Sadeghi solution

For $t > t_{PUR}$ the infiltration rate f_{SA} using the solution by Sadeghi et al. [7] is calculated as follows:

$$a = \Psi_f(\theta_s - \theta_i) \quad (4)$$

$$t_s = \frac{a}{K_S}\left[\frac{P(t_{PUR})}{a} - \ln\left(1 + \frac{P(t_{PUR})}{a}\right)\right] \quad (5)$$

$$t_{ga} = t - t_{PUR} + t_S \quad (6)$$

$$c_{SA1} = 1.4127 + 0.6843\sqrt{1 + 2 \cdot \frac{9.43456a}{K_S \cdot t_{ga}}} \quad (7)$$

$$c_{SA2} = \frac{2a}{K_S \cdot t_{ga} \cdot c_{SA1}} \quad (8)$$

$$f_{SA}(t) = K_S(1 + c_{SA2}) \quad (9)$$

B. Implementation of the Serrano solution

The implementation of the solution by Serrano [5] follows the same steps the Sadeghi implementation up to equation (6). The infiltration rate f_{SE} is then calculated using:

$$c_{SE1} = K_S \cdot t_{ga} + P(t_{PUR}) \quad (10)$$

$$c_{SE2} = \frac{c_{SE1}+a}{P(t_{PUR})+a} \quad (11)$$

$$c_{SE3} = \frac{a}{c_{SE1}+a} \quad (12)$$

$$c_{SE4} = c_{SE1} + a\ln(c_{SE2})\left(1 + \frac{c_{SE3}}{(1-c_{SE3})(1+c_{SE3}\ln(c_{SE2}))}\right) \quad (13)$$

$$f_{SE}(t) = K_S\left(1 + \frac{a}{c_{SE4}}\right) \quad (14)$$

C. Implementation of Travert

Travert et al. [6] implemented an integral approach that does not explicitly consider the ponding time. The infiltration rate f_{TR} is calculated by:

$$c_{TR}(t) = P - F(t-1) \quad (15)$$

$$f_{TR}(t) = K_S\left(1 + \frac{a + c_{TR} \cdot (\theta_s - \theta_i)}{F(t-1)}\right) \quad (16)$$

It should be noted that the derivation and use of c_{TR} in this implementation is not entirely clear to us. We think it is linked to accounting for an increased infiltration due to the hydrostatic pressure head from ponded water. However, c_{TR} should then also be set to the actual water depth.

D. Infiltration Parameters

In TELEMAC, the K_S value can be defined spatially variable. The suction head, initial water content and saturated water content are defined as a spatially constant value in the steering file. To further assess the impact of the spatial inhomogeneity of soils, we have extended all implementations to account for the spatial variability of all infiltration parameters.

In examining the equations used in the Sadeghi and Serrano solutions, Equation (4) provides a convenient means to combine the suction head, initial water content, and saturated water content into a single parameter, a. This parameter is then read directly from the geometry file.

For the Travert implementation, Equation (16) has been modified to include the spatial variability of $\Delta\theta$, defined as:

$$\Delta\theta = \theta_s - \theta_i \quad (17)$$

The additional spatial variability of infiltration parameters is only applied in the test case of the catchment in Germany.

E. Infiltration after the Rain Event

A key advantage of the Green-Ampt infiltration model is its ability to simulate continuous infiltration after rainfall has ceased. Specifically, if the infiltration capacity exceeds the current rainfall, ponded water on the surface can continue to infiltrate into the soil.

At the end of the subroutine "runoff_greenampt.f" the variable "PLUIE%R" is computed. This variable is then added to the source terms in the subroutine "prosou.f". The value of "PLUIE%R" is determined by subtracting the infiltration capacity from the current rainfall, thereby allowing for the infiltration of ponded water when it takes on negative values.

The Sadeghi and Serrano solutions have been implemented to account for this post-rainfall infiltration process. The implementation by Travert has also been extended to include this capability. However, it should be noted that we did not conduct a comprehensive analysis to verify whether this extension is entirely consistent with the initial infiltration process as implemented in Travert's method.

III. The Pluie Test Case

A. Test Case Description

The *pluie* test case confines a 100 m x 100 m square domain with a constant elevation and closed wall boundaries. Within this domain, four distinct K_S values are assigned (see Figure 1). For better interpretability, all K_S values as well as other rainfall and infiltration parameters are expressed in mm/h. The test case is driven by a hyetograph with hourly precipitation rates of 20, 30, 50, 100, 30, and 20 mm, respectively, resulting in a cumulative rainfall of 250 mm over six hours (Figure 2, although the highest intensity is truncated for visibility). The simulations extend for an additional hour beyond the precipitation event to observe post-rainfall infiltration dynamics.

We compare four different implementations of the Green-Ampt infiltration model: the solutions by Sadeghi and Serrano, the original implementation by Travert, and our extended version of the Travert implementation that accounts for the infiltration of ponded water.

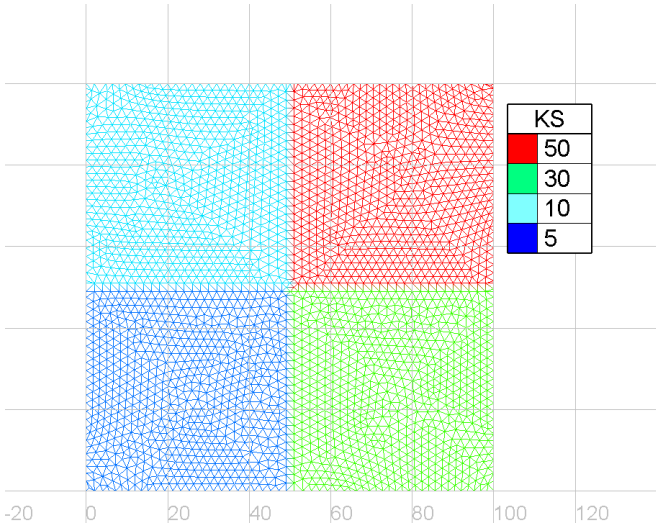

Figure 1. The mesh of the pluie test case with four different K_S values in mm/h.

B. Results

As long as the rainfall intensity is lower than the K_S value, all precipitation is infiltrated into the soil and no runoff occurs. If the rainfall intensity is larger than the K_S value, full infiltration continues until the ponding time is reached. After that, the infiltration capacity declines until it reaches the K_S value.

This behavior is evident in the implementations of the Sadeghi and Serrano solutions, as depicted in Figure 2. The infiltration capacities at the region with K_S= 30 mm/h align with the rainfall intensity (indicated by the dotted line) during the first two hours. In the third hour, as the rainfall intensity surpasses the K_S value, ponding occurs almost immediately. The Sadeghi solution exhibits a considerably higher infiltration capacity compared to the Serrano solution, although both solutions converge to nearly identical values by the end of the simulation. Consequently, the accumulated infiltration for the Sadeghi solution is marginally higher than that for the Serrano solution (see Figure 3).

The Travert implementation does not restrict infiltration capacity based on rainfall intensity during the first two hours (see Figure 2), yet this does not have an effect on the accumulated infiltration (see Figure 3). After ponding occurs, the Travert implementations demonstrate higher infiltration capacities than the Sadeghi and especially Serrano solutions. Notably, the infiltration capacity in the Travert implementation increases during the fourth hour, following a rise in rainfall intensity to 100 mm/h, exceeding the boundary box of Figure 2, and only begins to decline after the rainfall intensity decreases.

Starting from the fifth hour, a divergence between the original and extended Travert implementations becomes apparent. In the original Travert implementation, infiltration capacity once again exceeds rainfall intensity, causing actual infiltration to be limited by rainfall intensity (as evidenced by the reduced slope of accumulated infiltration in Figure 3). In contrast, the extended Travert implementation, which allows ponded water to infiltrate, shows a more rapid decrease in infiltration capacity compared to the original. After the rainfall ceases, the original Travert implementation cannot infiltrate the ponded water, resulting in constant infiltration capacity and accumulated infiltration during the seventh hour (Figure 2 and Figure 3).

All these trends are consistent with the regions with different K_S values.

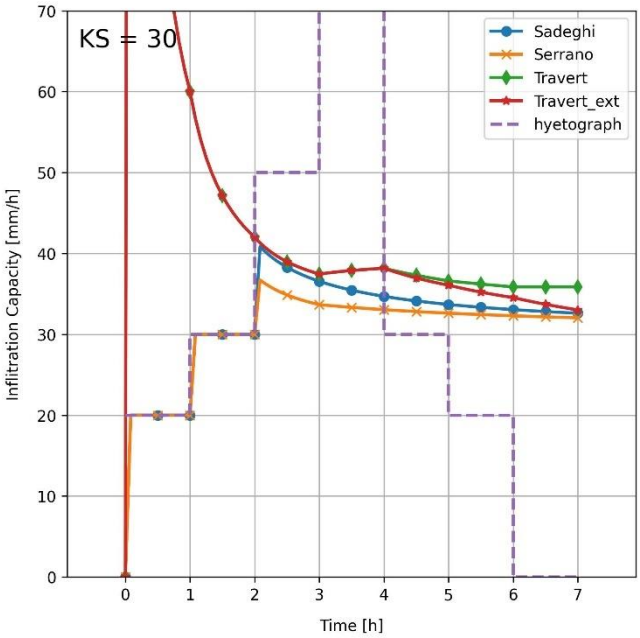

Figure 2. Calculated infiltration capacities by the four implementations for the region with K_S =30mm/h. Additionally, the hyetograph is depicted. In the fourth hour, the rainfall intensity of 100 mm/h exceeds the boundary box of this figure.

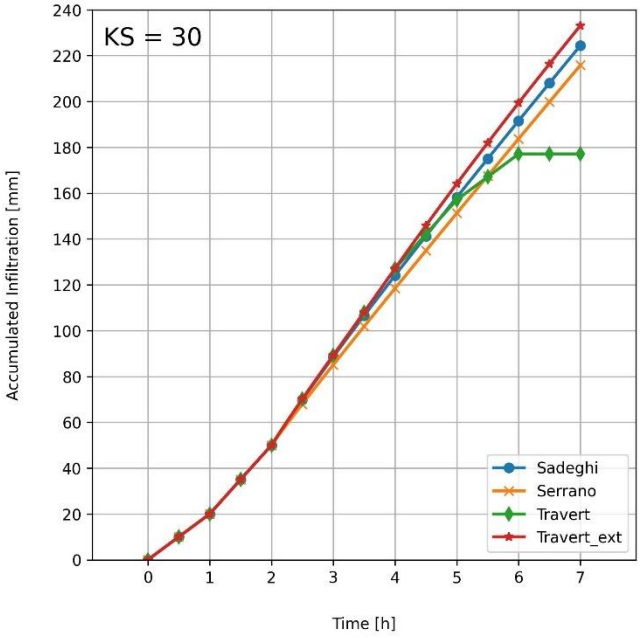

Figure 3. Calculated accumulated infiltration by the four implementations for the region with K_S =30mm/h.

Figure 4 presents the resulting water depths for the four implementations. Due to the small size of the test case and its uniform elevation, significant spatial variations in water depth only manifest while dry regions still exist. This complicates the interpretation of Figure 4 during the initial hours of the simulation, as water flows from regions with lower K_S values to regions of higher K_S values.

However, distinct trends emerge after the peak of the hyetograph ($t = 4$ h). Notably, the water depth in the extended Travert implementation does not increase further following the peak rainfall intensity, but decreases and ultimately exhibits the lowest water depth at the end of the simulation. The water depths produced by the explicit solutions appear nearly parallel, with the Serrano solution resulting in slightly higher depths compared to the Sadeghi solution. Conversely, the original Travert implementation shows a continued rise in water depth during the rain event, which remains constant after the precipitation ceases. Consequently, this implementation results in the highest water depth at the conclusion of the simulation.

C. Discussion

The extended Travert implementation improves upon the original implementation by enabling additional infiltration of ponded water. However, the observed increase in infiltration capacity following the onset of ponding is not physically consistent. This anomaly is linked to the parameter c_{TR} in Equation (16), which directly incorporates the accumulated rainfall into the infiltration capacity calculation. Setting this parameter to 0 omits this anomaly. This adjustment has been preliminarily validated using a simple Python script, although it has not yet been rigorously tested within the TELEMAC framework.

Comparatively, the infiltration capacity calculated using the Serrano solution is lower than that derived from the Sadeghi solution. Detailed analysis of the infiltration capacity at each simulation timestep reveals that the Serrano solution introduces a discrete drop in infiltration capacity immediately after ponding begins. In contrast, the Sadeghi solution results in a more gradual transition, reflecting a smoother and potentially more realistic infiltration process.

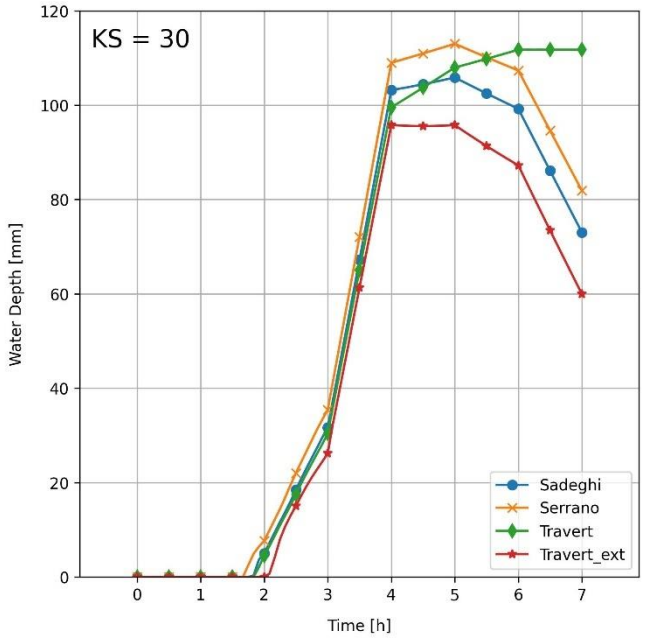

Figure 4. Resulting simulated water depths for all four implementations for the region with K_S =30mm/h.

IV. The Heigelsbach Test Case

This second test case examines whether the different implementations of the Green-Ampt infiltration method yield significantly divergent results when applied to flash flood modeling on a catchment scale.

A. Test Case Description

The selected test area is the Heigelsbach catchment, spanning approximately 58 km² in Northern Bavaria, Central Germany. The catchment drains into the Main River and features elevations ranging from 370 meters at the headwaters to 170 meters at the confluence (see Figure 5). The catchment's land use includes forested areas to the west and agricultural land to the south and east, with several villages dispersed throughout. The lower reaches, near the confluence, are part of the suburban area of Würzburg.

Particular attention was given to the generation of the computational mesh. Buildings located near channels were represented in the mesh as holes (see Figure 6), whereas buildings further away from the channels were not considered in the mesh generation. Overland flow areas are modeled with elements having an edge length of 15 meters, while the primary and secondary channels were modeled with finer elements ranging from 0.5 to 1.5 meters in edge length (see Figure 6).

In 2D hydrologic-hydrodynamic flash flood modeling on a catchment scale, it is crucial to accurately incorporate hydraulic structures like culverts. Given that official culvert datasets are often incomplete, field surveys were conducted to identify and document missing culverts. Preprocessing scripts for generating culvert data from shapefiles or transferring culvert data from an existing mesh to a new one are available upon request from the corresponding author.

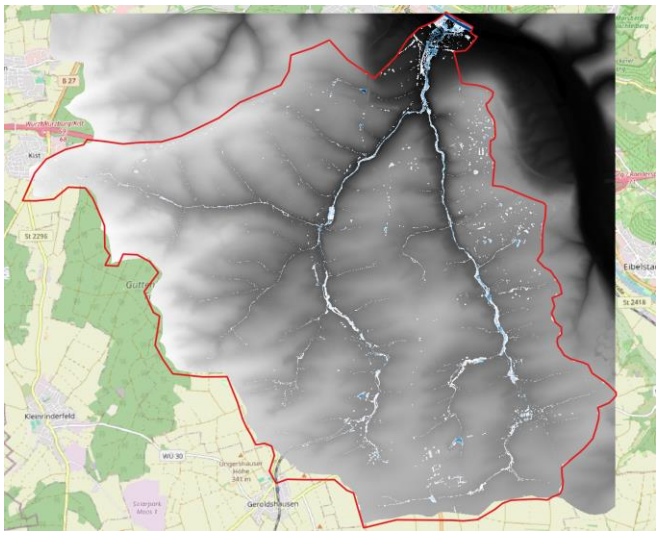

Figure 5. The second test case in Germany. The outline is shown with the red polygon. The distribution of water during the flash flood is shown on top of the topography raster.

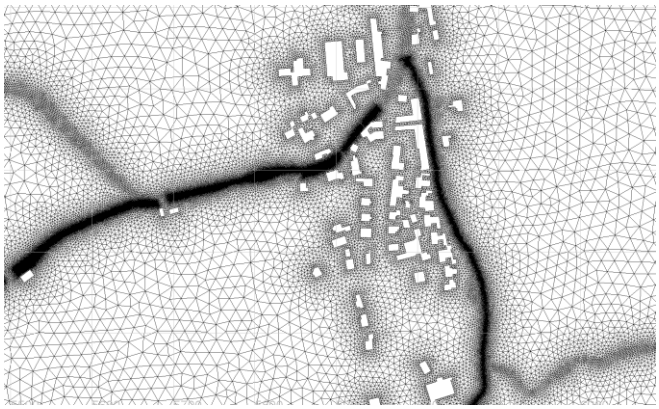

Figure 6. Exemplary display of the mesh with holes from buildings and mesh refinement in main and secondary channels. Refinement gaps within the main channels point to culverts being present there.

The hydrologic parameters for the Green-Ampt infiltration are sourced from a spatially refined data set developed by Mitterer [10]. Two scenarios are investigated:

- First Scenario: Only the K_S value is spatially variable, while the suction head, the initial water content, and the saturated water content are held constant at the spatially averaged value across the catchment.
- Second Scenario: all infiltration parameters are defined as spatially variable.

In both scenarios, the rainfall event modeled represents a 100-year return period storm with a four-hour duration, following an Euler II distribution, totaling 61 mm of precipitation. Hydrographs are extracted for the Heigelsbach at a location just upstream of its entry into the suburban area. Given that the catchment is ungauged, no calibration data are available.

B. *Results First Scenario – Spatially Variable K_S Only*

Figure 7 illustrates the hydrographs of the Heigelsbach for the different implementations under the first scenario. The Serrano implementation produces the highest peak discharge with 132 m³/s, followed by the Sadeghi implementation at 117 m³/s, the original Travert implementation at 115 m³/s and the extended Travert implementation at 98 m³/s. Notably, the original Travert implementation exhibits substantially higher discharge values during the recession limb of the hydrograph, a result of its limited infiltration capability. The differences in peak discharge and recession behavior among the implementations are pronounced and significant.

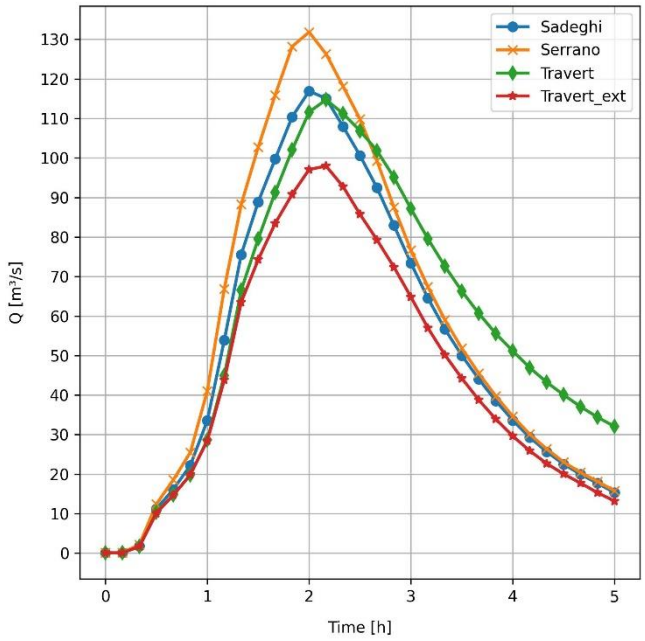

Figure 7. Comparison of the hydrographs of the Heigelsbach for different implementations with spatially variable K_S values and the other infiltration parameters kept constant.

C. *Results Second Scenario – all Infiltration Parameters Spatially Variable*

The infiltration parameter a from Equation (4) is spatially highly variable within the test area having a standard deviation of 0.70 cm with an average value of 1.37 cm. Still, allowing all infiltration parameters to vary spatially does not significantly alter the model outcomes. Figure 8 presents the hydrographs for the Sadeghi implementation under both scenarios; once with only K_S spatially variable and once with all infiltration parameters spatially variable. The differences are more noticeable in the ascending limbs of the hydrographs, yet the peak discharges differ by less than 1 m³/s. Similar trends are observed in the other implementations.

D. *Discussion*

Given the absence of calibration data, the conclusions drawn from this test case are inherently qualitative. The trends observed in the *pluie* test case are consistent with those seen here; the Serrano implementation results in the highest discharges, while the extended implementation by Travert yields the lowest.

The current model of the Heigelsbach still requires further refinement The decision to omit buildings that are not adjacent to the main channels may be justifiable from a hydrodynamic perspective, but it can lead to inaccuracies in hydrologic modeling. In the infiltration dataset, building areas are defined as sealed, meaning they are assigned a $K_S = 0$, preventing any infiltration. However, precipitation on building roofs is typically managed by storm drainage systems and does not contribute directly to surface runoff. Future model revisions should either include all buildings or incorporate alternative methods to accurately represent sealed areas.

Another issue highlighted by this case study is the definition of ponding conditions. Currently, ponding is triggered solely by rainfall. A more comprehensive implementation should consider triggering ponding due to inundation from overland flow as well.

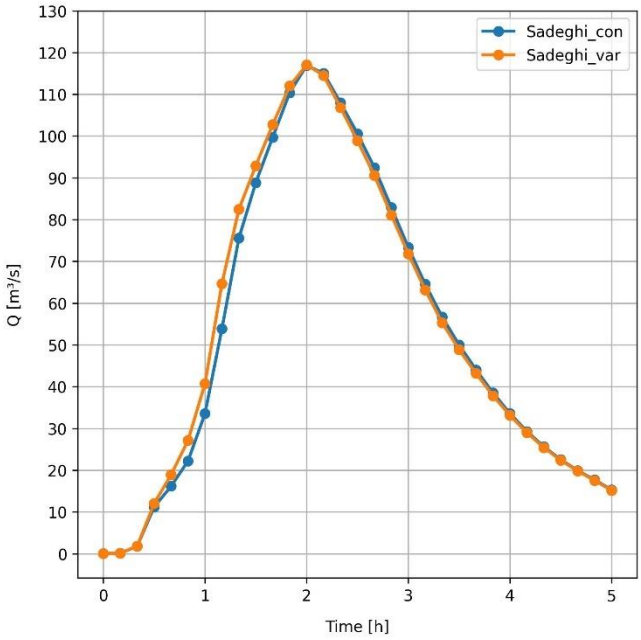

Figure 8. Comparison of the hydrographs of the Heigelsbach for the Sadeghi implementation. Once with only the K_S values spatially variable and once with all infiltration parameters spatially variable.

V. Conclusions and Outlook

Our simulations demonstrate that the choice of Green-Ampt infiltration method implementations significantly affects model outcomes. Among the explicit solutions, the Sadeghi implementation is preferable due to its smooth infiltration rate transition post-ponding. Conversely, the Travert integrative implementation shows an anomalous increase in infiltration rates following ponding when rainfall intensifies, likely due to the parameter c_{TR}. This might be fixed by revising the implementation (especially setting the parameter $c_{TR} = 0$). Extending the Travert implementation as described in this study allows for the infiltration of both rain and ponded water.

Future work will focus on applying the Green-Ampt infiltration method within TELEMAC to gauged catchments, which will enable robust model calibration and validation.

ACKNOWLEDGEMENT

We thank the German Ministry for education and research to support this study by funding the project Inno_MAUS. We furthermore want to thank the city of Würzburg and the LfU Bayern for providing detailed topography, land use, and infrastructure data.

A special thanks goes to Benedikt Schulz, who contributed to the first assessments of the Green-Ampt infiltration method in TELEMAC within his master thesis.

REFERENCES

[1] P.-L. Ligier, "Implementation of a rainfall-runoff model in TELEMAC-2D", Proceedings of the XXIIIrd TELEMAC-MASCARET User Conference 2016, Paris, France, pp. 13-19.

[2] U.S. Department of Agriculture, "National Engineering Handbook, Section 4, Hydrology, Chapter 10: Estimation of direct runoff from storm rainfall", Washington D.C., USA, 1972.

[3] K. Broich, T. Obermaier, L. Alcamo and M. Disse, "TELEMAC as a hydrodynamic rainfall-runoff model: New extension using the Green-Ampt-infiltration", Proceedings of the XXVIIIth TELEMAC User Conference 2022, Paris, France, pp. 143-145.

[4] W. H. Green and GA Ampt, "Studies on Soil Phyics", The Journal of Agricultural Science 4.1, 1911, pp. 1–24.

[5] S. E. Serrano, "Improved decomposition solution to Green and Ampt equation", Journal of Hydrologic Engineering, 8(3), 2003, pp. 158-160.

[6] J.-P. Travert, F. Taccone and V. Bacchi, "Modelling runoff for extreme rainfall events on large catchments using TELEMAC-2D", Proceedings of the XXVIIIth TELEMAC User Conference 2022, Paris, France, pp. 131-139.

[7] S. H. Sadeghi, H. W. Loescher, P. W. Jacoby and P. L. Sullivan, "A simple, accurate, and explicit form of the Green-Ampt model to estimate infiltration, sorptivity, and hydraulic conductivity", Vadose Zone Journal, 23(4), 2024.

[8] S. T. Chu, "Infiltration During an Unsteady Rain", Water Resources Research, 14(3), 1978, pp. 461-466.

[9] R. G. Mein and C. L. Larson, "Modeling Infiltration during a Steady Rain", Water Resources Research, 9(2), 1973, pp. 384-394.

[10] J. Mitterer, "Enabling Comparative and Reproducible Flash Flood Modeling Research in Bavaria - Local Contributions to a Global Objective", Munich, Germany, 2024.